



This open access document is published as a preprint in the Beilstein Archives with doi: 10.3762/bxiv.2019.25.v1 and is considered to be an early communication for feedback before peer review. Before citing this document, please check if a final, peer-reviewed version has been published in the Beilstein Journal of Nanotechnology.

This document is not formatted, has not undergone copyediting or typesetting, and may contain errors, unsubstantiated scientific claims or preliminary data.

Preprint Title Fast Microwave-Assisted Synthesis of Copper Nanowires as Reusable High-Performance Transparent Conductive Electrode

Authors Aina Shasha Hashimi, Riski Titian Ginting, Siew Xian Chin, Kam Sheng Lau, Muhammad Amirul Nazhif Mohd Nohan, Sarani Zakaria, Chi Chin Yap and Chin Hua Chia

Article Type Full Research Paper

ORCID® IDs Chin Hua Chia - <https://orcid.org/0000-0002-5269-4070>

Fast Microwave-Assisted Synthesis of Copper Nanowires as Reusable High-Performance Transparent Conductive Electrode

Aina Shasha Hashimi¹, Riski Titian Ginting², Siew Xian Chin³, Kam Sheng Lau¹, Muhammad Amirul Nazhif Mohd Nohan¹, Sarani Zakaria¹, Chi Chin Yap⁴ and Chin Hua Chia^{*1}

¹Materials Science Program, Faculty of Science and Technology, Universiti Kebangsaan Malaysia, 43600 Bangi, Selangor, Malaysia

²Department of Physics, Faculty of Mathematics and Natural Science, University of Sumatera Utara, Medan, Indonesia

³ASASlpintar Program, Pusat PERMATApintar[®], Universiti Kebangsaan Malaysia, 43600 Bangi, Selangor, Malaysia

⁴Physics Program, Faculty of Science and Technology, Universiti Kebangsaan Malaysia, 43600 Bangi, Selangor, Malaysia

Email: Chin Hua Chia – chia@ukm.edu.my

* Corresponding author

Abstract

We report the microwave synthesis of copper nanowires (Cu NWs) by using alkylamine-mediated approach. Cu NWs with aspect ratio ~612 was successfully synthesized at 120 °C for 4 h. Purification process of Cu NWs was done via a simple

and fast centrifugation method using water-hydrophobic organic solvent system. The effect of purification on the performance of the fabricated transparent conductive electrode (TCE) films was investigated. Purified Cu NWs TCE showed a low sheet resistance of 35 Ω /sq with high transparency of 81% (at λ_{550} nm). Glacial acetic acid (GAA) treatment was applied to the Cu NWs films to improve their conductivity and transmittance. The high conductivity of the Cu NWs TCE can be easily restored by using a quick GAA treatment.

Keywords

Cu NWs film; hydrothermal; nanomaterials; oxidation; transparent conductive film

Introduction

Metal nanowires and nanocrystals have attracted the attention of many researchers for the applications such as sensors, catalysts, electrocatalysts, flexible and transparent electrodes, and supercapacitor electrodes, and batteries [1–3]. One-dimensional (1D) nanocopper in particular has received great attention due to its high electrical conductivity [4]. Cu is 100 times less expensive and 1000 times more abundant than its competitor material Ag [5,6]. Moreover, the conductivity of copper nanowires (Cu NWs) is almost as good as silver nanowires (Ag NWs) [7,8]. This shows that at an even lower cost, by replacing AgNWs with Cu NWs would be able to give comparable performance [9].

Among the many methods used to synthesize Cu NWs, aqueous-media reduction of Cu salts is one of the most popular approaches that has been widely studied by using different capping and reducing agents [7,10–13]. This is due to its advantages such as relatively mild reaction conditions, does not need a vacuum

process and highly scalable [14,15]. Microwave-assisted synthesis of Cu NWs was previously reported by Liu et al. [16] via hexadecylamine (HDA)-mediated method. In comparison to the conventional method, microwave heating possesses many advantages including consistent distribution of particles size, control over morphology, and uniform heating [17–19]. Microwave energy was remotely introduced into the chemical reactor and passing through reaction vessel's walls to achieve direct heating of the reactants and solvents [20], allowing rapid heating and fast reaction [21].

A high quality transparent conductive electrode (TCE) requires a coating layer which is nearly transparent, highly conductive, and durable. The two well-known materials used to fabricate high-performance electrodes are Indium Tin Oxide (ITO) and silver nanowires (Ag NWs). Recent research works on Ag NWs showed that Ag NWs-based transparent electrodes could compete with ITO [22–24]. Unfortunately, silver is scarce and highly priced, while ITO-based electrodes are brittle, expensive and not eco-friendly [25]. To study fundamental electrical and mechanical properties, Cu NWs with thin diameter and high aspect ratio have become an ideal material [26,27]. The great potential of Cu NWs-based transparent electrodes have been reported previously. For example, Mallikarjuna et al. [28] has prepared a Cu NWs flexible transparent electrode (FTE) with sheet resistance of 128 Ω /sq at transmittance > 95% using spray coating and treatment with photonic welding method. Zhang et al. [29] synthesized high aspect ratio Cu NWs (~5000) and the films exhibited high optical performance of 91% at low sheet resistance of 92 Ω /sq.

Most of the procedures used to fabricate TCEs using Cu NWs require high temperature post-processing treatments under inert atmosphere [30–32]. Therefore, a dipping method using GAA was introduced to remove copper oxide and residual organics [25,33,34] on the Cu NWs, which is simpler, shorter in treatment time, and

can be conducted at ambient condition. This greatly reduces the cost and time taken to make a TCE. GAA also does not oxidize copper surface, therefore it can be used to remove copper oxide without attacking the copper film [35]. This treatment is also suitable for the fabrication of heat sensitive devices [33]. In this study, we reported the synthesis of Cu NWs using a microwave reactor, by investigating the effect of temperature, reaction duration, capping agents, and reducing agents on the properties of the Cu NWs obtained. We also demonstrated a procedure for separating Cu NWs from Cu nanoparticles (Cu NPs) in the reaction mixture using multiphase separation process. The performance of the Cu NWs in the form of TCE was investigated. Furthermore, we reported the effectiveness of GAA treatment on Cu NWs films to maintain its high conductivity performance as TCE.

Results and Discussion

Characterization of Cu NWs

XRD Analysis

Figure 1 shows the X-ray diffractogram of Cu NWs synthesized at 120 °C for 4 h without post-treatment. The results showed three diffraction peaks of (111), (200) and (220) at $2\theta = 43.2^\circ$, 50.3° , and 74.2° , respectively. All diffraction peaks could be indexed to those of face-centered cubic Cu (JCPDS04-0836). The intense and sharp diffraction peaks suggested that Cu NWs are highly crystalline. Furthermore, there are no other peaks for impurity phases such as Cu_2O or CuO [30,36].

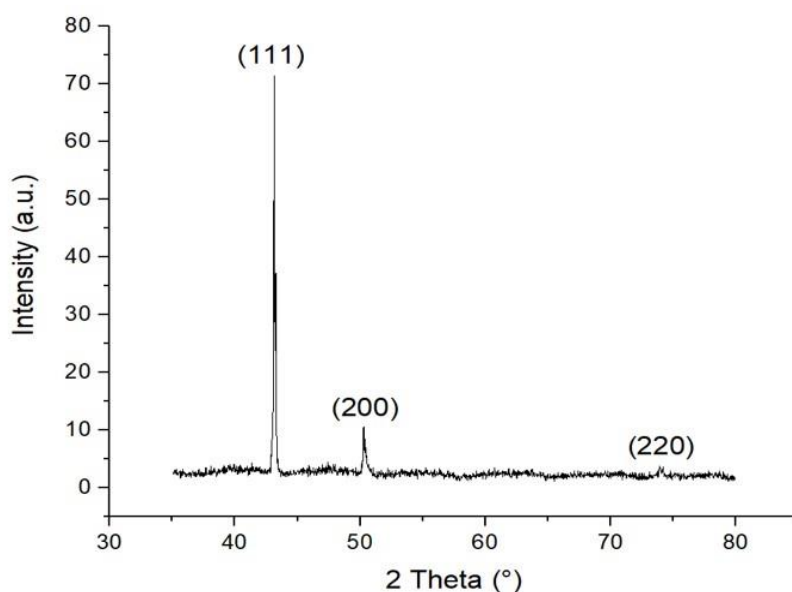


Figure 1: XRD diffractogram of Cu NWs obtained at 120 °C for 4 h.

Effects of Synthesis Time and Temperature on Growth of Cu NWs

Syntheses of Cu NWs were carried out at 120 °C for three different reaction times which were 2, 4 and 6 h. During the first 2 h of the synthesis process, only seeding was formed, based on the SEM image in Figure 2a. This can also be seen by the color of the product obtained, which was dark yellow. After 4 h, the color of the product was slowly changed to reddish brown which indicated the formation of Cu NWs [12,13,37]. After 6 h of synthesis time, the color of the products obtained still remained as reddish brown but slightly darker. Consequently, the grown Cu NWs at 6 h has almost identical aspect ratio to the ones synthesized at 4 h. Taking this into account, the optimum synthesis time of Cu NWs is 4 h.

Figure 2a–c and 2d show the SEM images of Cu NWs in low and high magnifications, respectively. Based on Figure 2a,b, it can be seen that Cu NWs formation did not occur until 4 h of synthesis time. At synthesis time of 4 h at 120 °C, Cu NWs with the highest aspect ratio of ~612 (length = $38 \pm 2 \mu\text{m}$ and diameter = $62 \pm 14 \text{ nm}$) were obtained. The growth of the Cu NWs can be explained by Ostwald

ripening process. This occurs when the small seeds recrystallized into relative large Cu nanoparticles during the reaction occur [29,38]. In the presence of capping agent, anisotropic growth is possible thus making it essential to control the morphology of NWs since it acts as the structure-directing agent by complexing with Cu(II) ion [39]. Organic capping ligands are normally involved in the important role of regulating the thermodynamics and 1D growth kinetics process [40,41]. Without capping agent, NWs could not be formed and this was shown by several studies [12,16,39].

Capping agents could prevent the twinned seeds from being oxidized and etched if the concentration is sufficient [5]. However, ODA which contains 18 carbons in the alkyl chain has very poor solubility in water [42]. The local concentration of the capping agent may be diminished due to the relative decrease of the alkyl amine's solubility. For the stabilization of initial seeds against situation like oxidative etching [43,44] this condition would be unfavorable and the seeds would probably grow to nanocubes or nanoparticles. Therefore, that is why there is coexistence of a relatively large number of nanoparticles along with NWs synthesized using ODA [44] which can be seen from Figure 2b,c.

The time taken for the ODA-mediated microwave-assisted synthesis of Cu NWs in this study was much shorter compared to previous studies [9,13,45] which used the conventional Teflon-lined autoclave method. In conventional heating, there is a temperature gradient from the surface to the inside because the material's surface needs to be heated first followed by the heat going inside. This is different from microwave heating since heat is generated throughout the reaction medium [21,46]. The rapid rise in temperature happened when the microwaves couple directly with the molecules of the whole reaction mixture. Instantaneous localized superheating of any substance that will respond to either ionic conduction or dipole rotation will occur since the process is not limited by the thermal conductivity of the vessel [47].

Next, in order to understand the importance of temperature in the synthesis of Cu NWs using microwave reactor, Cu NWs produced at three different synthesis temperatures of 80, 100 and 120 °C were also characterized. When the synthesis was done at 80 °C, the color of the product obtained was mint colored (Figure 2f). This color was quite close to the color of the product before the synthesis was done which was light blue (Figure 2e). Moreover, the color of the product obtained from the synthesis done in 100 °C was light yellow (Figure 2g) which also indicated that the nanowires have not formed yet. Based on the color of the products obtained, the syntheses that were done below 120 °C did not yield any CuNW. As can be seen from Figure 2h, the synthesis done at 120 °C yielded a reddish brown solution which shows that Cu NWs was successfully synthesized at this temperature. For anisotropic growth of nanowires, the specific facets could not be activated by lower temperature [16].

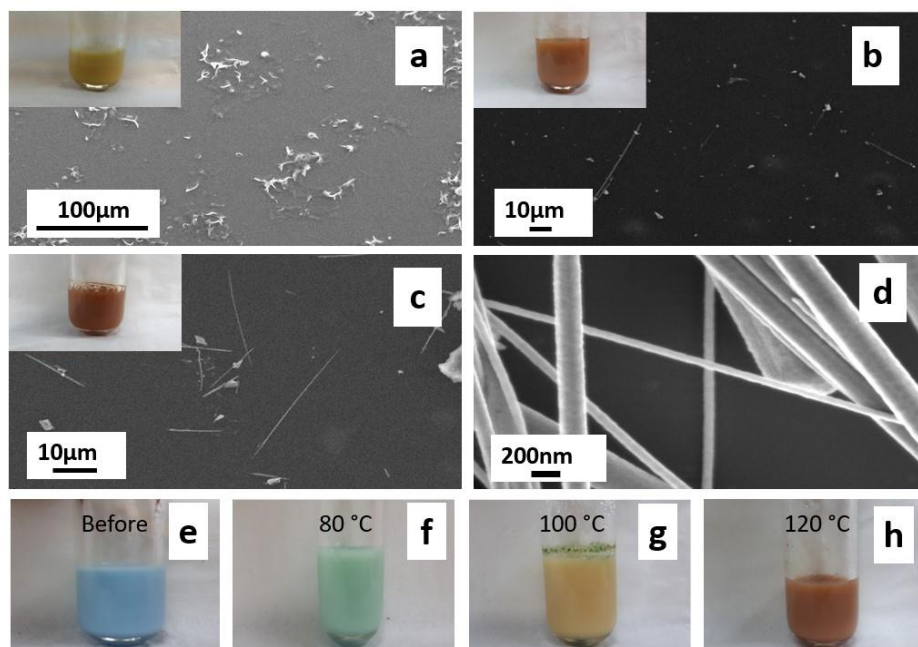


Figure 2: (a – c) SEM images of Cu NWs at synthesis time of 2, 4 and 6, respectively. The inset images are photographs of the products obtained at respective synthesis time; (d) High-magnification SEM image of Cu NWs at synthesis

time of 4 h; (e – h) Photographs of Cu solution corresponding to growth solutions of different synthesis temperature.

Effects of Different Capping and Reducing Agents

Several capping agents have been used in the synthesis of Cu NWs previously, such as hexadecylamine (HDA) [12], ethylenediamine (EDA) [48] and oleylamine (OLA) [8]. Among these capping agents, HDA is the most similar in terms of carbon length and solubility in water to ODA which is the capping agent used in this synthesis. Therefore, the experiment was also repeated using HDA as capping agent while maintaining other parameters to see the effects on the Cu NWs obtained. Based on Figure 3a, the synthesis using HDA as capping agent was successful with just 4 h of synthesis time, which is the same as the ones done using ODA.

Moreover, the experiment was also repeated using ascorbic acid as a reducing agent while maintaining other parameters. This was done to compare the Cu NWs produced in terms of physical structures using different reducing agents. Based on Figure 3b, it can be seen that the length of the Cu NWs were similar to the ones synthesized by using glucose. Overall, there wasn't much difference when comparing the results obtained from the synthesis between these two capping and reducing agents in terms of length of Cu NWs produced. This indicates that both capping and reducing agents can be used to synthesize Cu NWs.

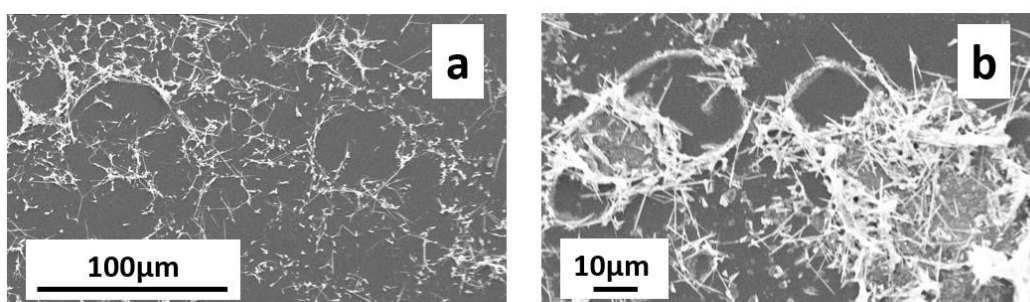


Figure 3: SEM images of Cu NWs synthesized using (a) HDA as capping agent and (b) ascorbic acid as reducing agent.

Mechanism of Cu NWs Purification Process

In previous studies, the purification of Cu NWs was done by several centrifugation processes and used many chemicals such as isopropyl alcohol, ethanol and n-hexane [12,49,50]. Due to the complicated and time-consuming conventional washing method, the multiphase separation method by using water-hydrophobic organic solvent system is more preferable due to shorter time and lesser amount of chemicals used. This purification method can be used to specifically purify Cu NWs that were synthesized using hydrophobic alkylamine such as HDA and ODA as the capping agent. As stated above, the synthesis of Cu NWs in this work uses ODA as capping agent which is an amphiphilic molecule that has a hydrophilic amino head and a long hydrophobic alkyl tail that contributes to its hydrophobicity [51,52]. Products of the synthesis of Cu NWs usually consist of NWs and undesired NPs, and the amount of NPs usually increased in larger reaction volume. This is due to the non-optimized mass/heat transfer during the synthesis process which was caused by the static reaction conditions that resulted in a less controlled nucleation and crystal growth [5,53]. Furthermore, in this study, the purification process was done using centrifugation method at 5,000 rpm for 10 min. This method is faster compared to waiting for the settling down of Cu NWs which took approximately 30 min.

Figure 4 shows the mechanism of the separation of Cu NWs and Cu NPs based on their surface properties as proposed by Kang et. al [51]. After addition of water and chloroform (CHCl_3), both of the solutions are phase-separated due to their immiscibility, in which CHCl_3 stayed below due to its higher density. As shown in

Figure 4a, due to the strong attraction between the long hydrophobic tails of ODA and CHCl_3 molecules, Cu nanostructures were covered with hydrophobic molecules which made them prone to stay in CHCl_3 . Even after the solution was sonicated for few seconds, Cu nanostructures still inclined to stay in CHCl_3 . When the solution was shaken, only a small amount of organics on the surface of Cu NWs dissolved into CHCl_3 (Figure 4b). This is due to the formation of NWs meshes that prevent the residual organics from directly contacting with CHCl_3 , and the twin defects existence in NWs which contributed to the stronger adsorption of twin boundaries to the capping agents [51,54]. On the other hand, the residual organics on the surface of Cu NPs were completely removed by CHCl_3 when the solution was shaken due to their monodispersity with organic solvents and weak adsorption to organic materials. Figure 4c shows that the force between residual organics and CHCl_3 that drives the NWs into CHCl_3 when the CHCl_3 reassembled below water. An aqueous film was formed on Cu NPs' surface due to the bonding of oxygen atoms of the water molecules with the bare Cu atoms [51]. As a result, the NPs that were surrounded by water were repelled by CHCl_3 and dispersed well in water. After the centrifugation process, NPs and NWs are settled at the bottom of water and CHCl_3 , respectively (Figure 4d).

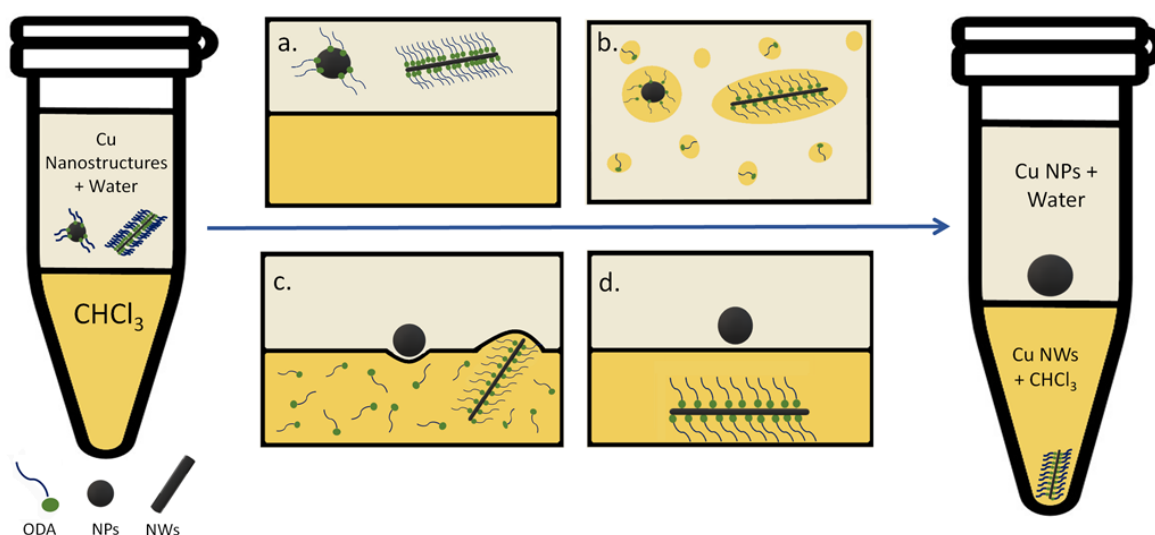


Figure 4: Schematic diagram of the mechanism of Cu NWs purification process.

Cu NWs Performance as TCEs

Before any treatment was done, the Cu NWs films showed a very high sheet resistance of 1 M Ω /sq and more. This might have been because upon exposure to air, copper forms a thin oxide layer [35]. Furthermore, capping agents such as HDA or ODA were still present on the surface of Cu NWs even after several washes and this was proven based on TEM images of Cu NWs obtained by Celle et al. [55]. The as prepared-Cu NWs films were not conductive unless the capping agent and oxides were removed. Generally, to remove residual organics or oxides, high annealing temperature under inert atmosphere was performed to make a highly conductive film. Unfortunately, the substrates used for TCEs applications which are usually polymers such as PET which could not withstand the high temperature annealing treatment [56].

In this study, GAA treatment was chosen as the post-processing treatment of TCE due to its simplicity and cost efficiency. Before the treatment was done, Cu NWs films showed very high sheet resistance due to the residual capping agent and oxide layer. After the films were dipped for 10 min in GAA solution, the sheet resistance reduced significantly from 1 M Ω /sq to ~35 Ω /sq. This proves that GAA treatment could largely improve the performance of Cu NWs TCEs. Figure 5a shows the plot of the comparison of transmittance (%) vs sheet resistance (Ω /sq) of Cu NWs films of this work and previously reported works [27,48,57,58]. From the inset images of Figure 5a(i,ii), it can be seen that the film was clearer and brighter after GAA treatment was done. This shows that besides increasing the conductivity of Cu NWs films, GAA treatment could also help in increasing the transmittance of the films [59]. The mechanism of the GAA treatment can be explained as follows. The

carboxylic acid species of GAA are likely to react with the amine groups of the remaining ODA. GAA could destabilize the copper–amine interaction by protonating the amine, thus promoting the dissolution of ODA in the liquid phase. At the same time, GAA could also remove the traces of copper oxides on the surface of Cu NWs, hence enhancing the conductivity of the nanowires [33]. As shown in Figure 5a, both of the transmittance and sheet resistance value decreased with the increased of Cu NWs density. This proves that the density of Cu NWs on the substrates strongly affects the performance of transmittance and conductivity of Cu NWs film [60,61]. In comparison to other references, the performance of Cu NWs TCE of this work is on par or slightly better with previous reports on Cu NWs films.

To show the importance of purification process on the performance of Cu NWs as TCE, both purified and unpurified Cu NWs were fabricated as TCEs and their performance were evaluated. As can be seen from Figure 5b, at similar sheet resistance values, the transmittance of unpurified Cu NWs films were lower than that of the purified Cu NWs. Performance of the purified and unpurified Cu NWs films of this work obtained for each concentration can be found in Table 1. The decrease in transmittance value was due to the presence of NPs in NWs which act as the center of light scattering. In addition, they do not contribute to the overall electrical conductivity due to their isotropic shape with poor connection on the percolating nanowire network [51,62,63]. Furthermore, it is very important to study the chemical stability of Cu NWs film. Cu is more susceptible to surface oxidation compared to Ag and Au due to its sensitivity to moisture and oxygen in the ambient atmosphere, and this causes performance degradation of CuNWs films [61]. Figure 5c shows a plot of a normalized $\Delta R/R_0$ where ΔR is the actual change in the sheet resistance and R_0 is the initial sheet resistance, versus time as an evaluation of stability. To avoid the influence of NWs density, both of the films have similar initial sheet resistance. From

Figure 5c, it can be seen that in ambient conditions, the Cu NWs film showed a low and almost steady sheet resistance over a period of 4 hours. On the other hand, the sheet resistance of Cu NWs film that was aged in an oven at 60 °C increased significantly due to the accelerated oxidation kinetics.

A critical problem of Cu NWs TCE is that it will be readily oxidized even when stored at room temperature, which can be seen from Figure 5c. Therefore it is important to find a way to restore the conductivity value of Cu NWs films to ensure its good performance as TCE. Hence, an experiment was done by re-dipping Cu NWs films in GAA after being aged in an oven at 60 °C for 90 min to evaluate the change in performance before and after treatment. Sheet resistance values were tested by using the four-point probe method. Figure 5d shows the plot of the sheet resistance of Cu NWs films before and after treatment with GAA, vs cycle numbers. The initial value from the first cycle is measured after GAA treatment done on Cu NWs film before inserted in the oven for testing. It can be seen that the sheet resistance of the film increased by ~10-fold of its initial value after 90 mins in the oven. After that, the film was taken out, dipped in GAA for 10 min and the sheet resistance was measured. Amazingly, the sheet resistance of Cu NWs films greatly reduced back to a value similar to its initial one, highlighting the ability of GAA to solubilize copper oxide which has superficially grown [33]. This experiment was repeated for five times and the conductivity of Cu NWs returned back to a value similar to its original each time. At the fifth cycle, the sheet resistance of Cu NWs film after treatment has a slight increase compared to the initial value. This is probably because Cu NWs was slightly washed away due to the multiple dipping in GAA solution [25].

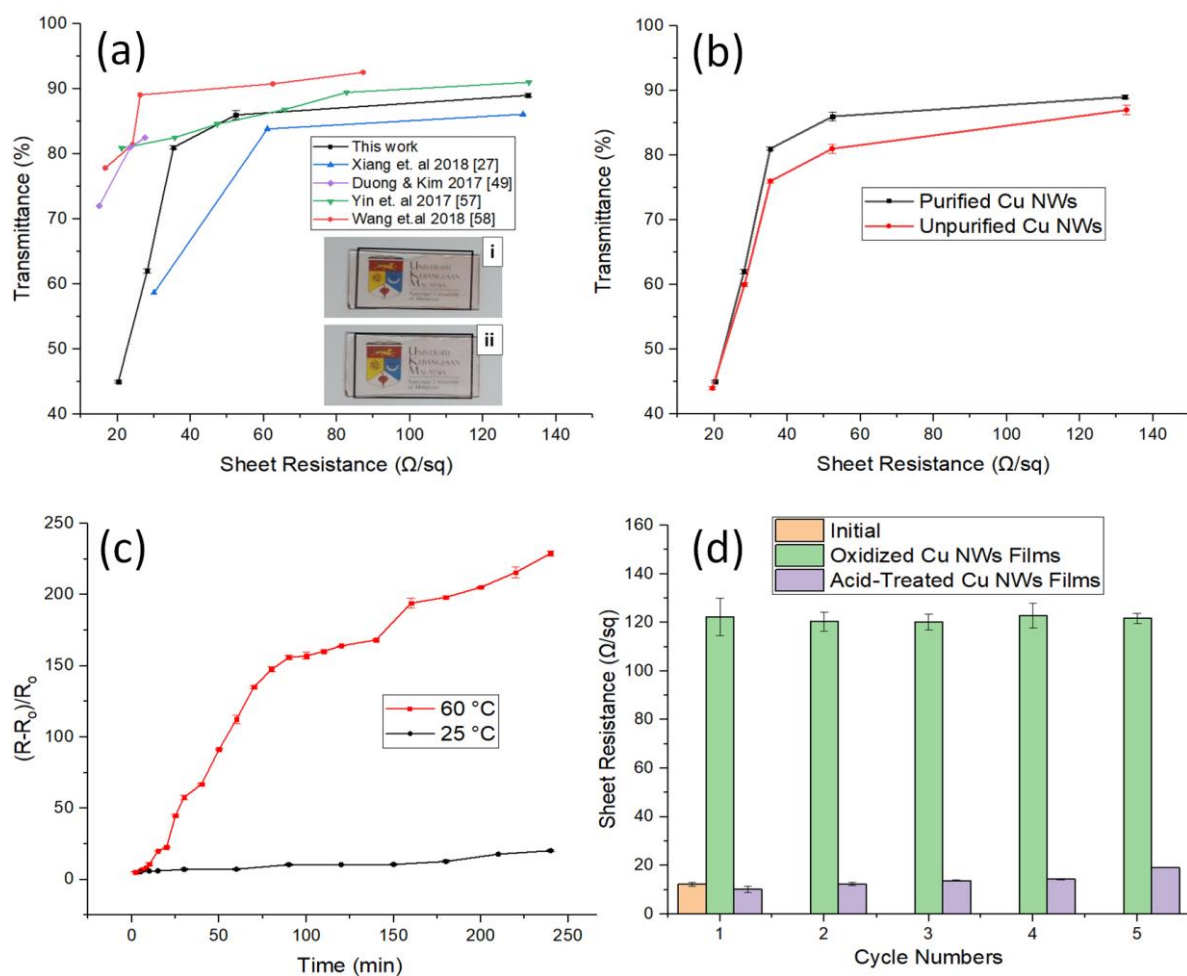


Figure 5: (a) Comparison of transmittance (%) vs sheet resistance (Ω/sq) of Cu NWs films between our study and previously reported studies. The inset images are Cu NWs film of this study of 89% transparency (i) before GAA treatment and (ii) after GAA treatment; (b) Performance of purified and unpurified Cu NWs films; (c) Plot of normalized sheet resistance of Cu NWs films vs time in a ambient conditions of 25 °C and in oven at 60 °C, and (d) Plot of sheet resistance of Cu NWs films vs time in a ambient conditions of 25 °C and in oven at 60 °C. Error bars represent the standard deviation values.

The electrical conductivity properties of Cu NWs was also analyzed using scanning spreading resistance microscopy (SSRM). SSRM is an AFM-mode mapping of topography and the local resistivity of the sample simultaneously [64].

Figure 6a shows the current mapping image of Cu NWs prior to GAA treatment. There was no current flow along the nanowire which can be seen by the empty spot in the middle of the image. This is probably due to the oxide and residual ODA layer on the surface of the Cu NWs. Figure 6b shows the current mapping image after the GAA treatment was applied. There was an increase in current flow of the Cu NWs TCE from 3.45 nA to 7.88 nA after GAA treatment, which can be attributed to the removal of unwanted layers on the surface of Cu NWs, thus improving its electrical conductivity. Next, the sample was aged in an oven at 60 °C for 45 min. After undergoing aging, the current flow along the sample decreased to 3.29 nA due to the formation of oxide layer on the surface of the Cu NWs thus preventing good electrical contact, and this can be seen from Figure 6c where the Cu NWs were no longer fully connected. The current flow increased significantly to 20.12 nA after the retreatment with GAA, which again proved the capability of GAA to remove the oxide layer. All of the results obtained from SSIMR analysis are consistent with the four point probe test. Figure 7a–c shows the schematic diagram of the oxidation process of Cu NWs, where it started from when the surface of Cu NWs oxidized to Cu_2O , and then to CuO and $\text{CuCO}_3 \cdot \text{Cu}(\text{OH})_2$. The second step dominates as Cu_2O layer thickens and this is because the first step will be limited due to the slow migration of Cu^+ and electrons [65].

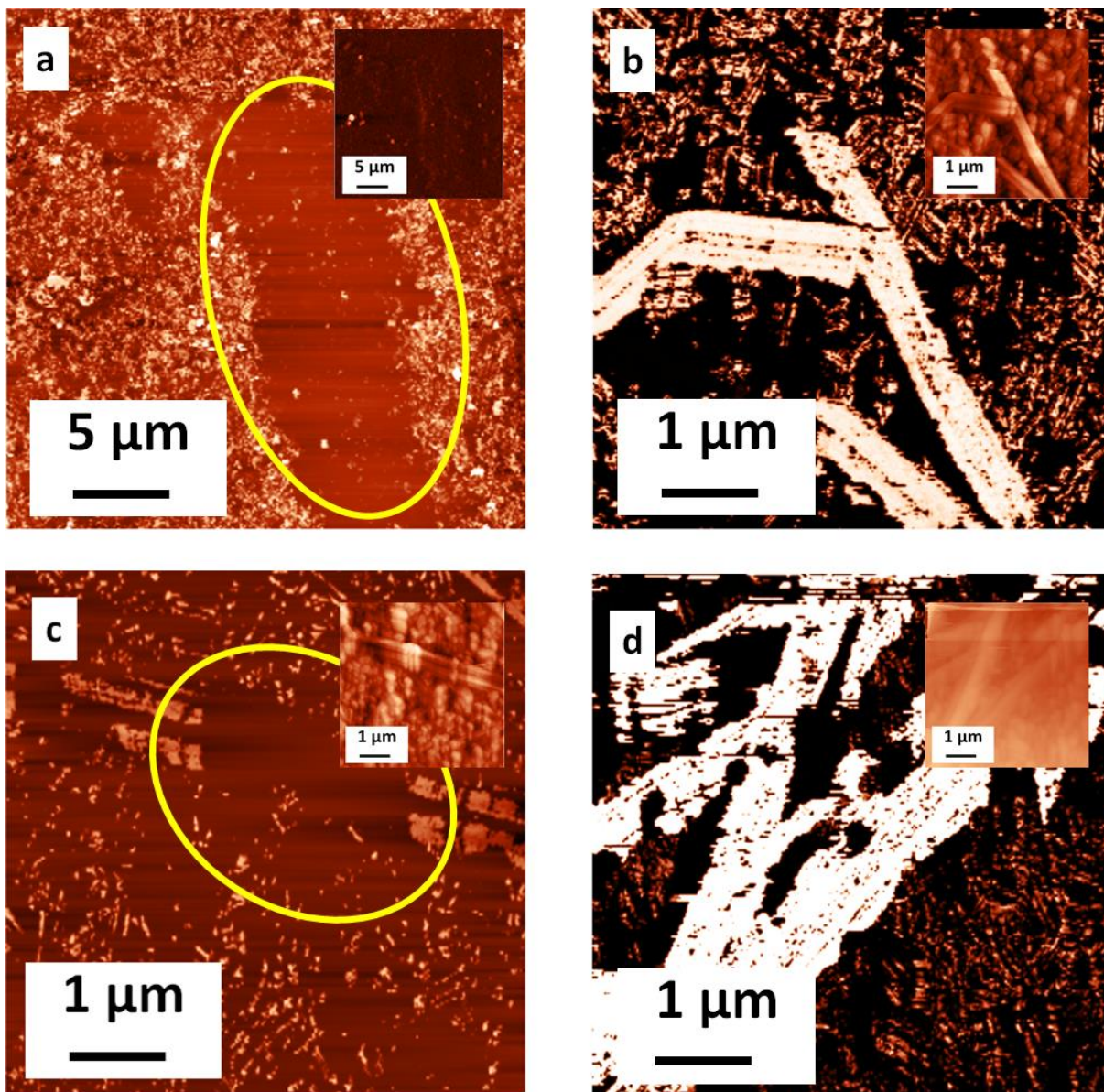


Figure 6: Current mapping image of (a) before GAA treatment (b) after GAA treatment (c) after aging in oven for 45 min at 60 °C, and (d) after retreatment with GAA. The inset images are the topography of each sample.

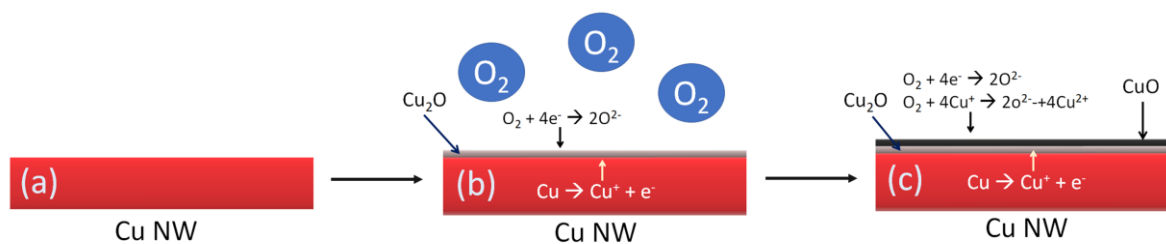


Figure 7: Schematic diagram of the oxidation mechanism of Cu NWs.

Table 1. Variation of sheet resistance and transmittance of purified and unpurified Cu NWs films of different concentrations.

| | | | | | |
|--|----|----|----|----|-----|
| Sheet resistance (Ω / sq) | 20 | 28 | 35 | 53 | 132 |
| Transmittance of purified Cu NWs (%) (at λ_{550} nm) | 45 | 62 | 81 | 86 | 89 |
| Transmittance of unpurified Cu NWs (%) (at λ_{550} nm) | 44 | 60 | 76 | 81 | 87 |

Conclusion

In summary, Cu NWs of aspect ratio ~612 was successfully synthesized using a microwave reactor, where ODA acts as capping agent and glucose as reducing agent. Our results show that both time and temperature play a significant role in the reaction and strongly influence the formation of Cu NWs. The purification process of CuNWs was done by using a simple centrifugation method of water-hydrophobic organic solvent system. Moreover, fabrication of Cu NWs TCE showed a low sheet resistance of 35 Ω /sq at high transparency of 81% (at λ_{550} nm) after being treated with GAA for 10 min. The purification process also proved to be an important step which can influence the performance of Cu NWs TCEs. Furthermore, Cu NWs film showed a stable performance when stored under ambient conditions and GAA treatment was still applicable to restore the high conductivity of Cu NWs films that have been oxidized.

Experimental

Materials

Copper chloride dihydrate ($\text{CuCl}_2 \cdot 2\text{H}_2\text{O}$, $\geq 99.0\%$), octadecylamine (ODA, $\text{C}_{18}\text{H}_{39}\text{N}$, $\geq 85.0\%$), 2-Propanol (IPA, $\text{C}_3\text{H}_8\text{O}$, $\geq 99.8\%$) and chloroform (CHCl_3 , $\geq 99.8\%$) were obtained from Merck. Glucose ($\text{C}_6\text{H}_{12}\text{O}_6$, $\geq 99.5\%$) was obtained from Sigma. Glacial acetic acid (GAA, CH_3COOH , 99.85%) was obtained from HmbG Chemicals. All chemicals were used as received. All solutions were prepared with deionized water.

Synthesis of Cu NWs

To synthesize Cu NWs, 0.8 mmol $\text{CuCl}_2 \cdot 2\text{H}_2\text{O}$ and 2.0 mmol ODA were mixed in a 30 mL deionized water and heated at 65 °C in a water bath for one hour. The light blue colored solution was sonicated for one hour. After that, 0.4 mmol glucose was dissolved in 30 mL deionized water. Both solutions were added in a G30 vial and then placed into a microwave synthesis reactor (Anton Paar Monowave 300). We used different synthesis times (2, 4 and 6 h) and temperatures (80, 100 and 120 °C). After that, a reddish brown solution was obtained and washed using the method outlined by Qian et al. (2016) [36]. The remaining precipitate was dispersed and stored in chloroform. Lastly, the experiment was repeated using HDA and ascorbic acid as capping agent and reducing agent, respectively.

Purification Process of Cu NWs

The purification of Cu NWs was carried out in several simple steps using the method outlined by Qian et al. (2016) [36]. Firstly, the as-prepared Cu NWs were centrifuged at 10,000 rpm for 10 min. Second, CHCl_3 and water were added into the solution containing Cu nanoproducts and was sonicated for ~5s. Next, the solution was centrifuged at 5,000 rpm for 10 min. After 10 min, red precipitates can be seen at the bottom of the centrifuge tube, which are Cu NWs aggregates. The supernatant and

CHCl₃ were removed using a pipette. The Cu NWs were washed with CHCl₃ again and were stored in the refrigerator.

Fabrication of Cu NWs TCE

All glass slides used in the preparation process were cleaned under ultrasonic bath with deionized water, ethanol, and acetone for 10 min each. Cu NWs were dispersed in chloroform at different solid contents. Next, the Cu NWs suspension was spread evenly on top of a glass slide using a spin coater in ambient condition. After that, each glass slide was treated using 10% GAA solution (GAA : IPA = 1 : 9) by dipping method for 10 min.

Oxidation Stability and Reusability Test of Cu NWs TCEs

For oxidation stability test, the fabricated Cu NWs film were tested under two conditions which were ambient condition and high-temperature aging. For the ambient condition test, the samples were left in ambient air at 25 °C for 4 hours. For the high temperature aging test, the samples were heated at 60 °C in an oven for 4 hours. Calculation of $\Delta R/R_0$ where ΔR is the actual change in the sheet resistance and R_0 is the initial sheet resistance is done to assess the stability. Next, the reusability test was done by measuring the sheet resistance of Cu NWs film that was put into the oven of 60 °C for every 90 min. This test was repeated for five consecutive cycles. The sheet resistances of all samples were measured using the four-point probe method.

Characterization

The morphology of Cu NWs samples was analyzed by a scanning electron microscope (SEM, Cosem EM-30AX PLUS). The chemical composition and crystal

structure of the samples were examined by X-ray diffraction (XRD, Bruker D8 Advance) under Cu K α radiation. The sheet resistance of the TCE samples was measured using a four-point probe method with a source meter (Keithley 2401). Transmittance spectra were measured using UV-vis spectrophotometer (Jenway 7315). The topography and current imaging of the sample was analyzed by a NT-MDT Scanning Probe Microscope (SPM) model NTEGRA Prima.

Acknowledgements

The authors would like to thank the Centre of Research and Instrumentation (CRIM), UKM for the research grant (GUP-2017-055) provided.

References

1. Harsojo, H.; Puspita, L. A.; Mardiansyah, D.; Roto, R.; Triyana, K. *Indones. J. Chem.* **2017**, *17*, 43–48. doi:10.22146/ijc.23618.
2. Ginting, R. T.; Ovhal, M. M.; Kang, J. W. *Nano Energy* **2018**, *53*, 650–657. doi:10.1016/j.nanoen.2018.09.016.
3. Kim, S.; Yun, T. G.; Kang, C.; Son, M. J.; Kang, J. G.; Kim, I. H.; Lee, H. J.; An, C. H.; Hwang, B. *Mater. Des.* **2018**, *151*, 1–7. doi:10.1016/j.matdes.2018.04.047.
4. Mohl, M.; Pusztai, P.; Kukovecz, A.; Konya, Z.; Kukkola, J.; Kordas, K.; Vajtai, R.; Ajayan, P. M. *Langmuir* **2010**, *26*, 16496–16502. doi:10.1021/la101385e.
5. Jin, M.; He, G.; Zhang, H.; Zeng, J.; Xie, Z.; Xia, Y. *Angew. Chemie - Int. Ed.* **2011**, *50*, 10560–10564. doi:10.1002/anie.201105539.
6. Nam, V. B.; Lee, D. *Nanomaterials* **2016**, *6*, 47. doi:10.3390/nano6030047.
7. Rathmell, A. R.; Wiley, B. J. *Adv. Mater.* **2011**, *23*, 4798–4803. doi:10.1002/adma.201102284.
8. Guo, H.; Lin, N.; Chen, Y.; Wang, Z.; Xie, Q.; Zheng, T.; Gao, N.; Li, S.; Kang, J.; Cai, D.; Peng, D.-L. *Sci. Rep.* **2013**, *3*, 2323. doi:10.1038/srep02323.
9. Ding, S.; Jiu, J.; Tian, Y.; Sugahara, T.; Nagao, S.; Suganuma, K. *Phys. Chem. Chem. Phys.* **2015**, *17*, 31110–31116. doi:10.1039/C5CP04582G.
10. Li, H.; Wang, L.; He, Y.; Hu, Y.; Zhu, J.; Jiang, B. *Appl. Therm. Eng.* **2015**, *88*, 363–368. doi:10.1016/j.applthermaleng.2014.10.071.
11. Ye, S.; Rathmell, A. R.; Stewart, I. E.; Ha, Y.-C.; Wilson, A. R.; Chen, Z.; Wiley, B. J. *Chem. Commun.* **2014**, *50*, 2562–2564. doi:10.1039/C3CC48561G.
12. Yoon, H.; Shin, D. S.; Babu, B.; Kim, T. G.; Song, K. M.; Park, J. *Mater. Des.* **2017**, *132*, 66–71. doi:10.1016/j.matdes.2017.06.042.
13. Ding, S.; Tian, Y.; Jiu, J.; Suganuma, K. *RSC Adv.* **2018**, *8*, 2109–2115. doi:10.1039/C7RA12738C.
14. Guangming, W.; Dan, L.; Jianxiang, Y.; Dongdong, F. *Integr. Ferroelectr.* **2017**, *183*,

- 1–7. doi:10.1080/10584587.2016.1163167.
15. Koo, J.; Kwon, S.; Kim, N. R.; Shin, K.; Lee, H. M. *J. Phys. Chem. C* **2016**, *120*, 3334–3340. doi:10.1021/acs.jpcc.5b10733.
 16. Liu, Y.-Q.; Zhang, M.; Wang, F.-X.; Pan, G.-B. *RSC Adv.* **2012**, *2*, 11235–11237. doi:10.1039/c2ra21578k.
 17. Jhung, S. H.; Jin, T.; Hwang, Y. K.; Chang, J. S. *Chem. - A Eur. J.* **2007**, *13*, 4410–4417. doi:10.1002/chem.200700098.
 18. Bi, Y.; Nautiyal, A.; Zhang, H.; Luo, J.; Zhang, X. *Electrochim. Acta* **2018**, *260*, 952–958. doi:10.1016/j.electacta.2017.12.074.
 19. Pan, L.; Liu, S.; Zhang, X.; Oderinde, O.; Yao, F.; Fu, G. *J. Alloys Compd.* **2018**, *737*, 39–45. doi:10.1016/j.jallcom.2017.11.343.
 20. Shah, J. J.; Mohanraj, K. *Indian J. Pharm. Sci.* **2014**, *76*, 46. doi:10.4103/0250-474X.128606.
 21. Oghbaei, M.; Mirzaee, O. *J. Alloys Compd.* **2010**, *494*, 175–189. doi:10.1016/j.jallcom.2010.01.068.
 22. Bai, S.; Wang, H.; Yang, H.; Zhang, H.; Guo, X. *Mater. Res. Express* **2018**, *5*, 026406. doi:10.1088/2053-1591/aaab26.
 23. Wang, S.; Tian, Y.; Ding, S.; Wang, C. *Mater. Res. Express* **2016**, *3*, 075007. doi:10.1088/2053-1591/3/7/075007.
 24. Liu, Y.; Chen, Y.; Shi, R.; Cao, L.; Wang, Z.; Sun, T.; Lin, J.; Liu, J.; Huang, W. *RSC Adv.* **2017**, *7*, 4891–4895. doi:10.1039/c6ra27760h.
 25. Tran, N. H.; Thinh, D. V.; Trinh, X. L.; Hoang, H. M.; Kim, H. C. Flexible transparent electrode fabrication by using copper nanowires. In Proceedings of the Proceedings of ISER 139th International Conference; 2018; pp. 6–9.
 26. Ye, E.; Zhang, S. Y.; Liu, S.; Han, M. Y. *Chem. - A Eur. J.* **2011**, *17*, 3074–3077. doi:10.1002/chem.201002987.
 27. Xiang, H.; Guo, T.; Xu, M.; Lu, H.; Liu, S.; Yu, G. *ACS Appl. Nano Mater* **2018**, *1*, 3754–3759. doi:10.1021/acsanm.8b00722.
 28. Mallikarjuna, K.; Hwang, H. J.; Chung, W. H.; Kim, H. S. *RSC Adv.* **2016**, *6*, 4770–4779. doi:10.1039/C5RA25548A.
 29. Zhang, Y.; Guo, J.; Xu, D.; Sun, Y.; Yan, F. *Langmuir* **2018**, *34*, 3884–3893. doi:10.1021/acs.langmuir.8b00344.
 30. Deshmukh, R.; Calvo, M.; Schreck, M.; Sologubenko, A. S.; Niederberger, M. *ACS Appl. Mater. Interfaces* **2018**. doi:10.1021/acsami.8b04007.
 31. Kim, H.; Choi, S. H.; Kim, M.; Park, J. U.; Bae, J.; Park, J. *Appl. Surf. Sci.* **2017**, *422*, 731–737. doi:10.1016/j.apsusc.2017.06.051.
 32. Zhu, Z.; Mankowski, T.; Balakrishnan, K.; Shikoh, A. S.; Touati, F.; Benammar, M. A.; Mansuripur, M.; Falco, C. M. *ACS Appl. Mater. Interfaces* **2015**, *7*, 16223–16230. doi:10.1021/acsami.5b01379.
 33. Mayousse, C.; Celle, C.; Carella, A.; Simonato, J.-P. *Nano Res.* **2014**, *7*, 315–324. doi:10.1007/s12274-013-0397-4.
 34. Duong, T.-H.; Kim, H.-C. *Ind. Eng. Chem. Res.* **2018**, *57*, 3076–3082. doi:10.1021/acs.iecr.7b04709.
 35. Chavez, K. L.; Hess, D. W. *J. Electrochem. Soc.* **2001**, *148*, G640–G643. doi:10.1149/1.1409400.
 36. Biçer, M.; Şişman, I. *Powder Technol.* **2010**, *198*, 279–284. doi:10.1016/j.powtec.2009.11.022.
 37. Wang, R.; Ruan, H. *J. Alloys Compd.* **2016**, *656*, 936–943. doi:10.1016/j.jallcom.2015.09.279.
 38. Yang, H.; He, S.; Tuan, H. *Langmuir* **2014**, *30*, 602–610. doi:10.1021/la4036198.
 39. Tan, M.; Balela, M. D. *Adv. Mater. Res.* **2015**, *1119*, 34–37.

- doi:10.4028/www.scientific.net/AMR.1119.34.
40. Bhanushali, S.; Ghosh, P.; Ganesh, A.; Cheng, W. *Small* **2015**, *11*, 1232–1252. doi:10.1002/sml.201402295.
 41. Bol'shagin, E. Y.; Roldughin, V. I. *Colloid J.* **2012**, *74*, 649–654. doi:10.1134/S1061933X12060038.
 42. National center for biotechnology information. PubChem compound database; CID=15793; [cited 2018 October 20]. Available from: <https://pubchem.ncbi.nlm.nih.gov/compound/15793> Available online: <http://pubchem.ncbi.nlm.nih.gov/compound/1983#section=Top>.
 43. Zheng, Y.; Zeng, J.; Ruditskiy, A.; Liu, M.; Xia, Y. *Chem. Mater.* **2014**, *26*, 22–33. doi:10.1021/cm402023g.
 44. Kumar, D. R. V.; Kim, I.; Zhong, Z.; Kim, K.; Lee, D.; Moon, J. *Phys. Chem. Chem. Phys.* **2014**, *16*, 22107–22115. doi:10.1039/C4CP03880K.
 45. Ding, S.; Jiu, J.; Gao, Y.; Tian, Y.; Araki, T.; Sugahara, T.; Nagao, S.; Nogi, M.; Koga, H.; Suganuma, K.; Uchida, H. *ACS Appl. Mater. Interfaces* **2016**, *8*, 6190–6199. doi:10.1021/acsami.5b10802.
 46. Yadoji, P.; Peelamedu, R.; Agrawal, D.; Roy, R. *Mater. Sci. Eng. B* **2003**, *98*, 269–278. doi:10.1016/S0921-5107(03)00063-1.
 47. Hayes, B. L. *Aldrichimica Acta* **2004**, *37*, 66–77.
 48. Duong, T.-H.; Kim, H.-C. *Int. Nano Lett.* **2017**, *7*, 165–169. doi:10.1007/s40089-017-0204-4.
 49. Jiang, Z.; Tian, Y.; Ding, S. *Mater. Lett.* **2014**, *136*, 310–313. doi:10.1016/j.matlet.2014.08.033.
 50. Liu, Y. Q.; Zhang, M.; Wang, F. X.; Pan, G. B. *RSC Adv.* **2012**, *2*, 11235–11237. doi:10.1039/c2ra21578k.
 51. Kang, C.; Yang, S.; Tan, M.; Wei, C.; Liu, Q.; Fang, J.; Liu, G. *ACS Appl. Nano Mater.* **2018**, *1*, 3155–3163. doi:10.1021/acsanm.8b00326.
 52. Li, W.; Tang, X. Z.; Zhang, H. Bin; Jiang, Z. G.; Yu, Z. Z.; Du, X. S.; Mai, Y. W. *Carbon N. Y.* **2011**, *49*, 4724–4730. doi:10.1016/j.carbon.2011.06.077.
 53. Qian, F.; Lan, P. C.; Olson, T.; Zhu, C.; Duoss, E. B.; Spadaccini, C. M.; Han, T. Y.-J. *Chem. Commun.* **2016**, *52*, 11627–11630. doi:10.1039/C6CC06228H.
 54. Xia, Y.; Xiong, Y.; Lim, B.; Skrabalak, S. E. *Angew. Chemie Int. Ed.* **2009**, *48*, 60–103. doi:10.1002/anie.200802248.
 55. Celle, C.; Cabos, A.; Fontecave, T.; Laguitton, B.; Benayad, A.; Guettaz, L.; Pélissier, N.; Nguyen, V. H.; Bellet, D.; Muñoz-Rojas, D.; Simonato, J. P. *Nanotechnology* **2018**, *29*, 085701. doi:10.1088/1361-6528/aaa48e.
 56. Guo, C. F.; Ren, Z. *Mater. Today* **2015**, *18*, 143–154. doi:10.1016/j.mattod.2014.08.018.
 57. Yin, Z.; Song, S. K.; Cho, S.; You, D. J.; Yoo, J.; Chang, S. T.; Kim, Y. S. *Nano Res.* **2017**, *10*, 3077–3091. doi:10.1007/s12274-017-1523-5.
 58. Wang, Y.; Liu, P.; Zeng, B.; Liu, L.; Yang, J. *Nano Res. Lett.* **2018**, *13*, 78. doi:10.1186/s11671-018-2486-5.
 59. Duong, T. H.; Tran, N. H.; Kim, H. C. *Thin Solid Films* **2017**, *622*, 17–22. doi:10.1016/j.tsf.2016.12.015.
 60. Li, S.; Chen, Y.; Huang, L.; Pan, D. *Inorg. Chem.* **2014**, *53*, 4440–4444. doi:10.1021/ic500094b.
 61. Chu, C. R.; Lee, C.; Koo, J.; Lee, H. M. *Nano Res.* **2016**, *9*, 2162–2173. doi:10.1007/s12274-016-1105-y.
 62. Pradel, K. C.; Sohn, K.; Huang, J. *Angew. Chemie Int. Ed.* **2011**, *50*, 3412–3416. doi:10.1002/anie.201100087.
 63. Gao, Q.; Kan, C.; Li, J.; Wei, J.; Ni, Y.; Wang, C. *Res. Chem. Intermed.* **2017**, *43*,

- 2753–2764. doi:10.1007/s11164-016-2793-3.
64. Celle, C.; Mouchet, C.; Rouvière, E.; Simonato, J. P.; Mariolle, D.; Chevalier, N.; Brioude, A. *J. Phys. Chem. C* **2010**, *114*, 760–765. doi:10.1021/jp9094326.
 65. Shi, L.; Wang, R.; Zhai, H.; Liu, Y.; Gao, L.; Sun, J. *Phys. Chem. Chem. Phys.* **2015**, *17*, 4231–4236. doi:10.1039/C4CP05187D.